The Effects of Temperature on One-dimensional Consolidation and Creep Behaviors of Hong Kong Marine Deposits

by

An LI

Department of Civil and Environmental Engineering

The Hong Kong Polytechnic University, Hong Kong, China

Email: an0929.li@connect.polyu.hk

Ze-Jian CHEN

Department of Civil and Environmental Engineering

The Hong Kong Polytechnic University, Hong Kong, China

Email: ze-jian.chen@connect.polyu.hk

Wei-Qiang FENG*

Department of Ocean Science and Engineering

Southern University of Science and Technology, Shenzhen, China

Email: fengwq@sustech.edu.cn

and

Jian-Hua YIN

Department of Civil and Environmental Engineering

The Hong Kong Polytechnic University, Hong Kong, China

Email: cejhyin@polyu.edu.hk

Abstract

The consolidation of Hong Kong marine deposits (HKMDs), a typical soft clayey soil in Hong Kong, is a serious concerned issue in engineering practices, such as coastal embankment construction and marine reclamations. Previous research works illustrate that high temperatures could accelerate the rate of consolidation of soft clayey soils, which has a great potential in future applications. Therefore, studies on the consolidation and stress-strain behaviors of clayey soils under varies thermal conditions are necessary. In this paper, a modified temperature-controlled oedometer has been developed and employed to investigate the effects of vertical stress and temperature on the consolidation and creep behavior of remolded HKMD with a temperature range of 20 to 60 °C. Scanning Electrical Microscopes (SEM) tests were performed to observe microstructure of HKMD specimens after oedometer tests under different temperatures. The results show that compression index C_c is nearly independent of temperature while swelling index C_s is slightly affected by thermal and stress path. As temperature increases, both permeability and coefficient of consolidation increase with the temperature and the time of end of primary consolidation is shortened. It is also found that the preconsolidation pressure decreases with an increase of temperature. Both linear and nonlinear creep functions are adopted to analyze the creep behavior and elevated temperature will reduce the linear creep rate and creep strain limit.

Keywords: temperature effect, nonlinear creep, consolidation, soft soils, permeability, creep strain limit

Introduction

The temperature effects on the properties and behavior of soils are of great concern in some specific conditions, including nuclear waste disposal, hot energy storage, energy piles, and buried electrical cables (Davies & Banerjee, 1980; Hueckel & Borsetto, 1990; Knellwolf et al., 2011; Amatya et al., 2012). The behavior of soils subjected to various temperatures will be changed accordingly. Furthermore, heating can be utilized to enhance the performance of vacuum prefabricated vertical drain (PVDs) preloading for soft soil ground improvement (Abuel-Naga et al., 2006). Thereby, a better understanding of the thermal-hydraulic-mechanical behaviors of soils is necessary.

To date, extensive laboratory investigations have been performed to study the 1-D mechanical properties and consolidation behavior of different soils under various temperatures. Previous works in the literature show that the permeability increases with temperature by both direct and indirect methods (Habibagahi, 1977; Towhata et al., 1993a; Delage et al., 2000; Abuel-Naga et al., 2005), whereas the intrinsic permeability appears to be not significantly affected by temperature (Delage et al., 2011). Previous studies indicate that the increasing hydraulic permeability results in an increase in the coefficient of consolidation (c_v) for most soils owing to the reduction of viscosity of pore water, transformation of free water from absorbed water, or soil skeleton revolution(Abuel-Naga et al., 2005; Jarad et al., 2019; Chen et al., 2022). Regarding the temperature effects on preconsolidation pressure, researchers found that various clayey soils show a decrease in preconsolidation pressure with increasing temperature. (Tidfors & Sällfors, 1989; Hueckel & Borsetto, 1990; Boudali et al., 1994; Moritz, 1995; C. Cekerevac et al., 2002; Cui et al., 2009; Hong et al., 2013).

The effect of temperature on the volume change behavior of soft soil has been investigated. Towhata et al. (1993a), Delage et al. (2004), Cekerevac and Laloui (2004), and Abuel-Naga et al. (2007) found that different types of normally consolidated (NC) soils showed irreversible volume contraction at high temperature and the over-consolidation ratio (OCR) has a significant impact on the thermally induced volume change for soft soils. Cekerevac and Laloui (2004) reported that the lightly over-consolidated soils exhibit thermally induced shrinkage, while the highly over-consolidated soils show expansion behavior upon heating. An abundance of different laboratory studies showed that the compression index (C_c) is independent of temperature (Campanella & Mitchell, 1968; Lingnau et al., 1996; H. Abuel-Naga et al., 2006; Li et al., 2018; Kaddouri et al., 2019; Chen et al., 2023), whereas the converse findings that C_c appears to decrease with heating were presented (Tang et al., 2008; Tsutsumi & Tanaka, 2012). Lingnau et al. (1996) and Tsutsumi and Tanaka (2012) found that the thermal effect on swelling index (C_s) is very slight. Nevertheless, Abuel-Naga et al. (2007) proposed C_s increases as temperature increases.

For the time-dependent behavior, extensive studies have been conducted and presented that the volumetric strain, strain rate and secondary consolidation coefficient increase with temperature increases (Gupta, 1964; Green, 1969; Towhata et al., 1993b; Fox & Edil, 1996; Burghignoli et al., 2000; Cui et al., 2009; Kaddouri et al., 2019). Unlike the above findings, Zhang et al. (2007) presented the results of triaxial creep tests which indicate the creep rate of axial strain increases as the soil samples were heated from ambient temperature up to 50 °C, whereas the creep rate decreases when the samples were subjected to the temperature of 60 °C. As mentioned above, the contradicting results presented in literature indicates that a systematic study for the investigation of thermal effect on clayey soils should be carried out.

In Hong Kong, due to the growth of infrastructure and the requirement for housing projects, an abundance of land area is demanded to fulfill the construction of civil structures and foundations (Yin, 1999b). Reclamation and building of artificial islands are efficient methods to relieve land pressure (Feng et al., 2017). Some reclamation projects, thereby, are or will be carried out in Hong Kong. Hong Kong marine deposit (HKMD) is one of the proposed fill materials to be backfilled or left in place as permanent disposal for reclamation projects. Its properties, such as low permeability, high compressibility, and low strength, may result in slow consolidation, excessive settlement, or bearing-capacity failure of the reclamation area backfilled with HKMD (Yin, 1999b). As described above, raising temperature may contribute to accelerating the consolidation of soft clayey soils, the PVDs-vacuum preloading combined with the heating has a broad application prospect in the ground improvement. However, the consolidation behavior of soft soils may be altered by these improvement techniques and the area of reclamation tends to exist in the remolded state for a long time. Despite numerous laboratory studies have been conducted on HKMD and most mechanical behavior of HKMD has been presented (Koutsoftas et al., 1987; Nakase et al., 1988; Zhu et al., 1999; Feng et al., 2017), there remains a need for investigating the properties and consolidation behavior of HKMC incorporating the effects of temperatures to fulfill the design requirements of reclamation projects or other geotechnical projects concerning the temperature fluctuation.

This study is to experimentally investigate the influences of temperature on the consolidation behavior of remolded HKMD. A series of multi-stage loading oedometer tests on HKMD under different temperature conditions was performed by employing a modified temperature-controlled apparatus. The results from oedometer tests demonstrated the characteristics of short-term behavior and long-term behavior. Several equations proposed in previous literature were verified by comparing the predicted results with experimental data. For the long-term behavior (*i.e.*, creep), the creep coefficient of each stress level was determined by the graphical method. The effects of temperature on the consolidation and creep behaviors of HKMD were analyzed. A nonlinear function proposed by Yin (1999a) was also adopted to evaluate the non-linear creep behavior of HKMD under different temperatures. Scanning electron microscope (SEM) tests were carried out on the specimens after oedometer tests at different temperatures to assist in the interpretation of the macroscopic behavior of HKMD from the microscopic perspective.

Experimental Program of the Temperature-Controlled Oedometer Tests

Material and Specimen Preparation

The original HKMD comprises shell, gravel, fine sand, silt, and clay particles with dark grey in color. It was collected from the location of a coastal area near Lantau Island in Hong Kong. The in-situ HKMD generally demonstrates high water content, low permeability, low shear strength, and high compressibility (Yin, 1999b; Fang & Yin, 2006). To obtain the consistent and uniform soil sample, the HKMD was sieved through 2 mm sieve.

Prior to the oedometer tests, the HKMD slurry with a water content of 110% was poured into a cylindrical steel bucket to complete self-weight consolidation. Then, additional vertical pressure from 5 to 28 kPa was gradually applied to the slurry for one-dimensional preconsolidation to obtain consistent soil specimens. When the preconsolidation was completed under the maximum pressure of 28 kPa, the soil was unloaded and five saturated HKMD specimens with a diameter of 70 mm and thickness of 19 mm were taken from the bucket with confining rings for all oedometer tests. Silicon grease was adopted to smear on the inner wall of confining ring to minimize the friction between the ring and soil specimen. Filter papers were placed on both the top and bottom sides of each specimen to prevent soil particles from entering the porous stones. Laboratory tests were carried out to determine the specific gravity, water content, Atterberg limits, and particle size distribution of soils in accordance with British Standard 1377. The basic physical properties of HKMD are summarized in Table 1. The particle size distribution curves obtained from the wet sieving and hydrometer test are shown in Fig. 1.

Modified Test Apparatus with Temperature-Control System

The oedometer tests were performed in a modified oedometer cell which allows constant temperature control from 20 to 70 °C. The modified oedometer comprises a Wykeham Farrance conventional oedometer, an electric heating wire, a temperature sensor, and a temperature controller unit. To avoid disturbing soil specimens, the temperature sensor with 0.1 °C resolution was placed in the annulus water surrounding the specimen to measure the temperature of the water to reflect the temperature in the soil specimen. This heating system could ensure that the water temperature is maintained within ± 0.1 °C of the set temperature throughout the test period. Fig. 2 shows the schematic diagram of the modified oedometer.

Since direct measurement of the internal temperature of soils may cause disturbance to specimens, calibration tests were conducted to determine the difference in temperature between soil specimens and surrounding water in the oedometer cell. During the working period of the heating system, two temperature sensors were inserted simultaneously into the center of the soil specimen and surrounding water respectively and maintained for 24 hours under a constant preset temperature. Subsequently, the positions of the temperature sensor inside the soil specimen were altered to investigate the uniformity of temperature inside the soil. The results of calibration tests show that the temperature of annulus water is approximately 2 °C higher than the temperature in the center soil specimen during the experimental testing and the temperature inside the soil specimen can be considered consistent. Meanwhile, the deformation induced by temperature and dead weight for each oedometer framework and apparatus was also carefully calibrated to reduce the error.

Test Program

In the thermo-PVDs-vacuum preloading improvement technique for reclamation projects or other high temperature-related geotechnical engineering, the temperature usually ranges from 20 to 70 °C (Shahrokhabadi et al., 2020; Chen et al., 2022; Chen et al., 2023). In view of this circumstance, the temperatures used in the modified oedometer tests in this study are in the range of 20 to 60 °C.

There are two groups with different temperature paths for oedometer tests. The first group aims to investigate the influences of temperature on the short-term and the long-term behavior of remolded HKMD at different constant temperatures, which is named the isothermal multi-stage loading (ITMSL) group. In this group, three oedometer tests were performed on the remolded HKMD specimens, namely group 1-Test 1 (G1T1), group 1-Test 2 (G1T2), and group 1-Test 3 (G1T3). Before applying the dead loading, the temperatures for the three tests were heated up to 20, 40, and 60 °C, respectively. At the prescribed temperature condition, the vertical stress was incrementally loaded to 400 kPa and decreased to 50 kPa at certain stress stages, and then reloaded to 1600 kPa. The details of loading procedures and durations are listed in Table 2. According to previous studies, the loading stages for creep lasted 7 days to ensure that there is sufficient time to observe the long-time behavior of HKMD (Yin, 1999a; Feng et al., 2017; Wu et al., 2020). The curves in terms of void ratio *versus* vertical stress ($e\text{-}log\sigma_z'$) for the three tests were plotted to determine the compression index (C_c), the swelling index (C_s), and the preconsolidation pressure (σ'_{zp}). The evolution of the vertical strain with the logarithmic scale of time (ε_z-$logt$) for each stage at different temperatures were also plotted to determine the time for end of "primary" consolidation (t_{EOP}) and creep coefficient ($C_{\alpha e}$). The consolidation coefficient and permeability (k_z) at each loading stage were also determined using the data from oedometer tests. The effect of temperature on these parameters mentioned above was investigated. In addition, Yin's non-linear creep function was employed to analyze the creep behavior at different constant temperatures.

The second group is the temperature-changed multi-stage loading path, which is also called the thermal path, involving applying elevated temperature to soil specimens under different vertical stresses. This group consists of two oedometer tests, namely group 2-Test 4 (G2T4) and group 2-Test 5 (G2T5), respectively. Similar loading procedures of group 1 were performed on G2T4 and G2T5, but the unloading-reloading stage was carried out at the vertical stress of 200 kPa to investigate the influence of vertical stress on the swelling index C_s. Most loading durations in group 2 for observing creep behavior are 10 days since each loading stage increase of 10 °C is a relatively small temperature change (Kaddouri et al., 2019). The difference between the two tests of group 2 is that, the temperature of G2T4 was increased by 10 °C at beginning of each loading stage before the unloading stage (from 50 to 200 kPa) until it was raised to 50 °C and then cooled to room temperature of 20 °C at the end of reloading stage of 200 kPa and the thermal path repeated at the begin of reloading stage of 400 kPa and G2T5 is a reference test with constant temperature of 20 °C. For the 5th stage, the loading duration is 1 day for G2T4 and 7 days for G2T5 since the creep strain induced by vertical stress only and combined effect of vertical stress and temperature could be compared. The objective of this group is to study the effect of the thermal path on the 1-D mechanical properties of

HKMD, including the preconsolidation pressure, the compression index, the swelling index, and the creep coefficient.

Results and Discussions

The effects of temperature on (*i*) consolidation coefficient and the time for end of "primary" consolidation, (*ii*) compression index and swelling index, (*iii*) preconsolidation pressure, (*iv*) permeability, and (*v*) creep behavior, are discussed in the following sub-sections.

The effect of temperature on the "primary" consolidation and coefficient of consolidation

Under the one-dimensional straining condition, the compression of soil consists of the "primary" consolidation and the creep, and the point of the end of "primary" consolidation (EOP) marks the transition between the two phases. Commonly, EOP is defined as the point when the excess pore pressure dissipates completely, and the continuous deformation (*i.e.,* creep) begins under the constant vertical stress. In this study, *Casagrande*'s logarithmic time method was adopted to determine the t_{EOP}. By using this approach, the values of t_{EOP} at certain stress levels for G1T1, G1T2, and G1T3 are determined and summarized in Table 3. The values of t_{EOP} for G1T1 range from 36 min to 82 min, which agrees well with previous research work on HKMD specimens with a height of 19 mm (Yin, 1999a; Cheng & Yin, 2005; Feng et al., 2017). Furthermore, it is found that the value of t_{EOP} is both stress-dependent and temperature-dependent. For any given loading stage, the value of t_{EOP} decreases at high temperatures, and it also decreases with increasing vertical stress at the same temperature. The results indicate that high temperature may have a positive effect on the dissipation of excess pore pressure, and thus accelerate the process of "primary" consolidation.

Figs. 3(a) and 3(b) depict the relationship between the incremental vertical strain $\Delta\varepsilon$ and time (log scale) of three isothermal tests under the vertical stress of 400 and 800 kPa, respectively. It is observed that the rate of consolidation increases with an increase in temperature, which is consistent with the findings of Abuel-Naga et al. (2005) and Jarad et al. (2019). To quantify the rate of consolidation, Taylor's square root of time fitting method was adopted to calculate the coefficient of consolidation, expressed as:

$$c_v = \frac{T_v H^2}{t} \tag{1}$$

where c_v is the coefficient of consolidation, H is the length of the longest drainage path, T_v is the vertical time factor, and t is the measured time. T_v is given as the following equation:

$$\text{For } U_v < 0.6,\ T_v = \frac{\pi}{4} U_v^2$$

$$\text{For } U_v > 0.6,\ T_v = -0.933\log(1-U_v) - 0.085 \tag{2}$$

where U_v is the average degree of consolidation. For U_v=98%, t in Eq. (1) is regarded as t_{EOP}. Thereby, the value of the coefficient of consolidation c_v for each vertical stress could be determined.

Fig. 4 illustrates the variations of the coefficient of consolidation with temperature. At any vertical stress level, the coefficient of consolidation c_v increases as temperature increases. To analyze the evolution of the value of c_v with temperature, the vertical stress level of 400 kPa for all isothermal tests is taken as an example for discussion. The c_v value of 8.06×10^{-8} m^2/s at 60 °C is 1.71 times larger than that at 20 °C, and the value of c_v at 40 °C is 6.27×10^{-8} m^2/s, which is 1.33 times larger than that at 20 °C. It can be seen that c_v increases with vertical stress increases at the same temperature level. Therefore, it could be inferred that the elevated temperature and higher vertical stress have a positive effect on the consolidation of HKMD.

The effect of temperature on permeability

It is widely accepted that the permeability of saturated clayey soil increases with temperature (Constantz, 1982; Towhata et al., 1993a; Delage et al., 2011; Jarad et al., 2019). The variation of hydraulic conductivity with the elevated temperature seems to be connected to several factors. Some researchers mainly attributed the increasing permeability to the decrease in the dynamic viscosity and density of the fluid in soils with temperature increases (Habibagahi, 1977; Ogawa et al., 2020). Reasonably, the thermal effect also alters the internal soil structure rearrangement, leading to the formation of the flow channels, which are conducive to free water flow (Constantz, 1982; Romero et al., 2001; Abuel-Naga et al., 2005). Apart from these two factors, an increase in temperature is able to facilitate the conversion of adsorbed water to free water so that the fluid in the soil could easily flow. Other factors that potentially affect the hydraulic conductivity incorporating the thermal effects are clay matrix, diffuse double layer thickness, and adsorbed water (Morin & Silva, 1984; Romero et al., 2001).

A large number of experimental works in the literature on the temperature impact on permeability have been reported. Few researchers adopted the constant head method as a direct method to measure the coefficient of hydraulic conductivity of clayey soils under various temperatures (Morin & Silva, 1984; Delage et al., 2000). Due to the difficulty of direct measurement for clay, a majority of scholars utilized the indirect method, which is to determine the coefficient of consolidation c_v and the coefficient of compressibility m_v by using the data obtained from oedometer or triaxial tests, so as to indirectly determine the permeability using the following equations:

$$m_v = \frac{H_i - H_f}{H_i} \cdot \frac{1000}{\sigma'_{vf} - \sigma'_{vi}} \tag{3}$$

$$k_z = m_v \gamma_w c_v \tag{4}$$

where m_v is the coefficient of compressibility, H_i is the heights of the specimen at each initial loading stage, H_f is the heights at the end of each loading stage, σ'_{vi} is the pressure applied to the specimen in the previous load increment, σ'_{vf} is the pressure applied to the specimen in the load increment, γ_w is the unit weight of water, and c_v is the coefficient of consolidation.

Taylor (1948) proposed a linear relationship between the void ratio and the logarithm of the permeability (*e-logk*) and C_k is defined as the slope of the linear curve, which is a permeability index. This finding was confirmed by many researchers. Fig.5(a) presents the variation of permeability with void ratio for three isothermal tests. It is found that the permeability increases with the temperature and the values of C_k are 0.568, 0.598, and 0.628, respectively. Furthermore, the relationship between C_k and temperature was plotted, which is shown in Fig. 5(b). It could be observed that the relationship is highly linear and a correlation for HKMD is e=0.0015log(k_z)+0.5382.

Considering that temperature apparently influences the properties of the fluid, such as the viscosity and the unit weight of pore water, the Kozeny-Carman equation is employed to appraise the permeability at certain temperature $k_z(T)$ based on the hydraulic permeability at room temperature $k_z(T_0)$, expressed as follow:

$$\frac{k_z(T)}{k_z(T_0)} = \frac{\mu(T_0)\gamma_w(T)}{\mu(T)\gamma_w(T_0)} \tag{5}$$

where $\gamma_w(T)$ and $\gamma_w(T_0)$ are the unit weight of pore water at certain test temperature and room temperature of 20 °C, respectively, $\mu(T_0)$ is the viscosity of pore water at 20 °C, and $\mu(T)$ is free water viscosity changed with temperature, which could be derived by following relation (Hillel, 1980):

$$\mu(T)=-0.0004657\ln(T)+0.00239138 \tag{6}$$

Fig. 6 compares the values of the hydraulic permeability obtained from the results of isothermal oedometer tests and the calculated results utilizing Eqs. (5) and (6). It can be observed that the permeability significantly increases with the temperature increases. Combined with Fig. 4, one can conclude that the increasing permeability upon heating significantly accelerate the consolidation of HKMD, which is in good agreement with the finding of pervious study (H. Abuel-Naga et al., 2006; Jarad et al., 2019). Owing to the reduction in viscosity of pore water, the absorbed water is much easier to transform into free water at higher temperature. Therefore, the consolidation rate increased and additional consolidation was generated, as shown in Fig. 3. It is also found that the calculated values of permeability also fit well with experimental data of oedometer tests at both 40 and 60 °C. Despite a good agreement between the calculated and experimental results, there are still a few deviations of calculated results from experimentally measured data. One possible reason is that the influence of temperature on the pore water viscosity may be altered by the salt concentration, which may be also related to the void ratio and the soil states.

The effect of temperature on compressibility characteristics

The typical compression curves in terms of void ratio and effective vertical stress of G1T1 at 20 °C at the time equal to t_{EOP} are shown in Fig.7. It is found the e-log $(\sigma_z^{'})$ curves for all five tests are well linear during the loading stage and unloading-reloading stage. As a result, it is effortless to graphically determine the values of compression index C_c and swelling index C_s

by fitting the experimental data in this study. All values of compress parameter, compression index, swelling parameter, and swelling index are calculated and summarized in Table 4. As shown in Fig. 7(a), the C_c value of G1T1 which is the slope of the normal compression line and the C_s value of G1T1 which is the slope of the swelling line in Fig. 7 are 0.153 and 0.0187, respectively, whose results agree well with the previous findings of similar soils (Yin, 1999b; Feng et al., 2017).

Fig. 8 shows the evolutions of compression index and swelling index with temperature for G1T1, G1T2, G1T3, and G2T4. Campanella and Mitchell (1968) first proposed that the value of C_c is independent of temperature, which has been verified subsequently by several researchers. Combined with Fig. 8 and Table 4, it appears that the compression index C_c is not affected significantly by either the high temperature or the thermal path. This concurred with previous findings. However, although the swelling index C_s is nearly unaffected by high constant temperature by comparing the results among G1T1, G1T2, and G1T3, it may be altered slightly by the heating-cooling cycle by comparing G2T4 and G2T5. Another observation from the results of G1T1 and G2T4 in Table 4 shows that the swelling index increases when the unloading stage is performed at high vertical stress. In general, upon the unloading-reloading circle, a strong mechanical degradation of the elastic modulus of soils could cause an increase in the swelling index C_s (Mohajerani et al., 2011). Therefore, the swelling index is related to loading history and thermal path, while it seems less concerned with a high constant temperature.

The effect of temperature on preconsolidation pressure

The preconsolidation pressure, which is an important behavior of both in-situ and remolded soils, is considered as the yielding point between elastic and plastic domains. Due to its significance in geotechnical engineering, the effect of temperature on preconsolidation pressure has been extensively investigated by many researchers (Eriksson, 1989; Tidfors & Sällfors, 1989; Hueckel & Borsetto, 1990; Boudali et al., 1994; Moritz, 1995; Abuel-Naga et al., 2005; Kaddouri et al., 2019). Fig. 9 depicts the evolution of preconsolidation pressure with temperature. Many of them found a reduction in preconsolidation pressure of various clayey soils with temperature increases.

As shown in Fig. 7, the value of $\sigma_{zp}^{'}$ can be estimated by employing the graphical method, which is the value at the intersection of two linear parts on the typical compression curve. Fig. 9 also presents the evolution of preconsolidation pressure of HKMD with temperature and the detailed values of $\sigma_{zp}^{'}$ of five HKMD specimens are also shown in Table 4. It is found that the samples of HKMD also show a decreased trend of the preconsolidation pressure with increasing temperature, which agrees well with the previous findings. However, the decreasing rate of the preconsolidation pressure with elevated temperature is not identical for different types of soils. It appears that $\sigma_{zp}^{'}$ decreases faster for the soils with a higher liquid limit with temperature increases. This could be described as the reduction of adsorbed water between clay particles owing to the much conversion of adsorbed water to free water at a higher temperature. Since the fluid in soils works as an elastic material between clay particles, the reduction of adsorbed water at high temperatures could contribute to the increase in mineral-to-mineral contacts, resulting in the generation of plastic strain and the decrease in the elastic domain (Tidfors & Sällfors, 1989).

Several empirical correlations have been proposed in the literature to predict the evolution of the σ'_{zp} as a function of temperature for soils. Boudali et al. (1994) performed a series of oedometer tests with various strain rates at different temperatures and proposed a linear relation between σ'_{zp} and temperature based on the experimental data. Whereas it is observed the change of preconsolidation pressure with temperature is not perfectly linear, which means that it decreases at a high rate and then tends to stabilization (refer to Fig. 9). Thereby, different non-linear functions to model the temperature effect on the evolution of σ'_{zp} were proposed by Hueckel and Borsetto (1990), Moritz (1995), and Cekerevac et al. (2002), as given in the following equations, respectively.

$$\sigma'_{zp}(T) = \sigma'_{zp}(T_0) + \alpha_1 \Delta T + \alpha_2 \Delta T \left| \Delta T \right| \tag{7}$$

$$\sigma'_{zp}(T) = \sigma'_{zp}(T) \left[\frac{T_0}{T} \right]^{\alpha} \tag{8}$$

$$\sigma'_{zp}(T) = \sigma'_{zp}(T_0) \left\{ 1 - \gamma \left[\log(T / T_0) \right] \right\} \tag{9}$$

where T_0 is the reference temperature, T is the current temperature, $\sigma'_{zp}(T_0)$ and $\sigma'_{zp}(T)$ are the preconsolidation pressure at T_0 and T, respectively, $\Delta T = T - T_0$ refers to the temperature difference, α_1 and α_2 are the parameters representing the sensibility of soils with respect to temperature for Hueckel's modified Cam-clay model, α is the model parameter for Moritz's equation, and γ is the parameter for Cekerevac's non-linear function.

The equations were adopted to evaluate σ'_{zp} incorporating the effect of temperature. Fig. 10 displays the predicted results of preconsolidation pressure with temperature increasing determined by utilizing Eq. (7), Eq. (8), and Eq. (9), and the predicted results are compared with the results obtained from the isothermal oedometer tests. It is noteworthy that the values of parameters α_1 and α_2 are equal to -0.1 and -0.0005 for Eq. (7), respectively, and the value of parameter α is equal to 0.11 for Eq. (8), and the value of parameter γ is 0.226 for Eq. (9). One can observe that the predicted results using aforesaid equations are in good agreement with the experimental results of HKMD. The predicted results using Eq. (7) could perfectly fit experimental results. Nevertheless, two parameters are cumbersome for modeling.

Cekerevac et al. (2002) noted that there is only a unique value for parameter γ for each type of soil and the parameter is related to the liquid limit of soils. Fig. 11 implies the evolution of the parameter with the liquid limit in literature. It could be deduced that the thermal effect on the preconsolidation pressure is dependent on the liquid limit: the soils with the higher liquid limit demonstrate the greater influence of temperature on $\sigma_{zp}^{'}$. The value of γ for HKMD was also presented together with the results of diverse types of soil with different liquid limits. Observation of the comparison from Fig. 11 discloses that the relationship is also applicable for HKMD with a liquid limit of 56%. In the subsequent constitutive model, thereby, the equation proposed by Cekerevac et al. (2002) is more suitable to predict the preconsolidation pressure as a function of temperature.

For group 2, since the temperature of the soil specimen for G2T5 was variational during the test period, the influence of temperature on the pre-consolidation pressure is not suitable for quantitative analysis using the above equations. But it could be seen that the preconsolidation pressure $\sigma_{zp}^{'}$ of the HKMC specimen that has gone through the thermal path decreased by 26.8% compared with that at room temperature of 20 °C. As a consequence, the temperature path and constant high temperature share a similar function, which makes the mineral-to-mineral contacts increase to reduce the preconsolidation pressure of HKMD.

The effect of temperature on creep behavior

As mentioned in the above section, the consolidation is divided into primary consolidation and creep. The creep refers to the continuous deformation under constant vertical effective stress. It is well acknowledged that creep occurs during and after the primary consolidation (Yin & Graham, 1989; Feng & Yin, 2017; Yin & Feng, 2017). Generally, the creep behavior is relevant to internal soil structure rearrangement, particle sliding, and viscous properties of soils. HKMD, as a typical soft clayey soil, is usually categorized as a problematical soil due to the excessive long-term settlement under surcharge load. The creep settlement of the HKMD is still an important issue that cannot be neglected in the aspects of the design and construction. Hence, the creep behavior of HKMD has been extensively studied (Yin, 1999b; Fang & Yin, 2006; Feng et al., 2017). The creep coefficient $C_{\alpha e}$ is widely adopted to analyze the creep behavior of clayey soils. Fig. 3(a) illustrates the determination of creep coefficient in ε-log$t$ plane and the function is expressed as:

$$C_{\alpha e} = \frac{-\Delta e}{\log(\Delta t)} \tag{10}$$

where Δe is the void ratio increment and Δt is the creep time.

For all oedometer tests in this study, the values of creep coefficient $C_{\alpha e}$ under different loading stages are determined by fitting the test data. The evolutions of the creep coefficient in terms of temperature for isothermal and temperature changed tests are depicted in Fig. 12.

From Fig. 12, it is observed that the creep coefficient tends to decrease with both increasing stress and temperature for HKMD. The results are in good agreement with the findings of Zhang et al. (2007) and Jarad et al. (2019). For the temperature changed test, it can be seen that the $C_{\alpha e}$ values of G2T4 under different vertical stress are larger than that of G1T2 (40 °C) and lower than G1T3 (60 °C). This is because that the highest temperature applied on the soil sample before 400 kPa stage was 50 °C. It might attribute to the temperature history effect on the microstructure of soil. When temperature is elevated, the temperature effects on the creep behavior of soil are complicated and it can be explained from several various aspects. First, the molecules will be more active to weaken the bonds between soil particles, which subserves internal soil structure rearrangement and particle sliding (Mitchell & Soga, 1976). Second, the reduction of pore water viscosity with an increase in temperature could contribute to the contraction of soils with time. Meanwhile, the diffuse double layer maybe decreases with the increasing temperature (Morin & Silva, 1984; Tidfors & Sällfors, 1989). However, the mechanisms of temperature influence on soils are not limited to the above. In general, elevated temperature acts in a similar way to the increase of vertical stress, making the internal structure of soil more stable and thus producing creep deformation (Yin, 1999a). Moreover, the mineral composition and content of different types of soil have contrasting responses to temperature. Therefore, these mechanisms work together on the soils and interact with each other, so that the creep coefficients of different soils show different responses to elevated temperature. In the following part, the results of SEM tests will act as an auxiliary method to support the mechanism analysis from the micro perspective.

Fig.13 displayed the creep strain of G2T4 and G2T5 with time under 50 kPa vertical stress. As illustrated in Table 2, G2T4 under 50 kPa stage was elevated to 30 ℃ and G2T5 was 20 ℃. It appears that the creep strain of G2T4 for 1 day is very closed to that of G2T5 for 7 days owing to the temperature effect, indicating that the increasing temperature causes additional creep strain under constant loading. It is also found the gap between two trend lines tends to increase with time, that reveals the creep strain rate is accelerated by the elevated temperature. Chen and Yin (2023) also reported that the creep strain and creep strain rate increase with temperature increases, which is consistent to the findings of this study.

Most conventional equations for analysis of the creep behavior are based on linear correlations between creep strain and the logarithm of time, including the model proposed by Yin and Graham (1989, 1994) which is expressed as:

$$\varepsilon_z = \varepsilon_{z0} + \frac{\psi}{V}\ln(\frac{t_0 + t_e}{t_0}) \tag{11}$$

where ε_{z0} is the initial strain at the time $t=t_0$, t_0 is the parameter implying the beginning of creep time, which is directly related to the strain rate on reference time line, t_e is equivalent time, ψ is the creep parameter that is constant for a given soil in this equation, and V is the initial specific volume, $V=1+e_0$.

The equation has been widely adopted to analyze the creep behavior. Nevertheless, one limitation of the linear creep function is that the strain calculated by Eq. (11) is infinite when t_e is equal to infinite. However, the clayey soils usually exhibit nonlinear creep behavior, and the secondary consolidation coefficient decreases with time (Yin, 1999a; Feng et al., 2017; Shi et al., 2018). Hence, a non-linear function has been proposed by Yin (1999a) to incorporate the influence of the decreasing creep parameter with time, expressed as:

$$\Delta\varepsilon_z = \frac{\psi_0 / V}{1 + \frac{\psi_0}{V\varepsilon_c^l}\ln[(t_0 + t_e)/t_0]}\ln[(t_0 + t_e)/t_0] \tag{12}$$

where ψ_0 is a material parameter, which is similar to creep parameter ψ, ε_c^l is the creep strain limit when the time is infinite, and the definitions of t_0 and t_e are the same as those in the linear function mentioned above. In this study, Yin's non-linear creep function was employed for the analysis of nonlinear creep behavior for HKMD at different temperatures. The effects of temperature on nonlinear creep parameter ψ_0 and creep strain limit ε_c^l were also discussed. To determine the values of ε_c^l and ψ_0, Eq. (12) can be given as:

$$\frac{\ln[(t_0+t_e)/t_0]}{\Delta\varepsilon_z}=\frac{V}{\psi_0}+\frac{1}{\varepsilon_c^l}\ln[(t_0+t_e)/t_0] \tag{13}$$

The values of t_0 are determined in advance in the curve-fitting process by using Eq. (13). Using an appropriate value of t_0 could plot a good fitting-curve with the data obtained from oedometer tests, while an inappropriate t_0 value may lead to incorrect nonlinear fitting parameters. Yin fitted the curves with the same values of t_0 (t_0=49 min) for different vertical stress levels and the fitting results agree well with the test results. Details can be referred to Yin (1999a). In this study, the t_0 values of all loading stages for the three isothermal oedometer tests are taken a constant value of 100 min, which can ensure all stages have finished the primary consolidation process.

Taking the HKMD specimen of G1T1 under the vertical stress of 1600 kPa as an example, a straight line in the space of $\ln[(t_0+t_e)/t_0]$ against $\ln[(t_0+t_e)/t_0]/\varepsilon_c^l$ was plotted and an equation of the form "*y=ax+b*" was determined, as presented in Fig. 14. The slope (*a*) of the straight line corresponds to $1/\varepsilon_c^l$ and the intercept (*b*) corresponds to V/ψ_0. Fig. 14 also illustrates and compares the results of curve fitting by using Eq. (13) for the three specimens in isothermal group under 1600 kPa. It could be seen that the values of curve fitting parameter R^2 are greater than 0.95, indicating the nonlinear creep function fits well with the experimental data obtained from creep tests.

The variations of creep strain limit ε_c^l and nonlinear creep parameter ψ_0 of three isothermal oedometer tests generated by curve fitting with Eq. (13) are shown in Fig. 15. It appears that under different temperature conditions (20 °C, 40 °C, and 60 °C), the value of both ψ_0 and ε_c^l decrease with the increasing vertical effective stress. The results are quite consistent with the previous findings (Yin, 1999a; Tong & Yin, 2011; Feng et al., 2017; Le et al., 2017). Similar to the variation of creep coefficient with the increasing temperature, it can be observed that both the nonlinear creep parameter and creep strain limit decrease as temperature increases. Based on the above results, the creep behavior and the non-linear parameters of HKMC could be seen as temperature dependent.

Microstructure interpretation

As mentioned above, SEM tests will provide the microstructural evidence of the oedometer tests. Fig. 16 presents the SEM photos of the three specimens after oedometer tests subjected to different temperatures in group 1 with 1000× and 3000× magnification. Figs. 16(a), 15(b), and 15(c) after binarization are also provided. The pores, particles, and morphological characteristics of soil aggregates are observed. It can be found, from Figs. 16, that the flocculated structure is the main microstructure, and the soil particles are mainly in the form of aggregates. It seems that the interaction between soil particles and aggregates in the G1T1 specimen is mainly characterized by face-to-face connection, while that in G1T2 and G1T3 specimens are dominated by the form of the face-to-face and line-to-face connection. The difference indicates that temperature will attribute to the soil particle rearrangement and the restructuring stage in soil microstructure. Comparing Figs. 16, it appears that, while the temperature increases, the contact between the particles is closer, the directionality gets much stronger, and the agglomerate morphology is more obvious. Meanwhile, one can observe that the microstructure of the specimen after oedometer test at room temperature is relatively loose, whereas the specimens get denser after heating treatment in oedometer condition.

The photographs show that as the higher temperature is subjected to soil specimens during 1D consolidation, the soil microstructure becomes denser, the interaction is changed to some extent, and the soil particle rearrangement is more complicated. These micro behaviors indicate that the vertical strain increases as the temperature increases (see Fig. 3). It also explains the above inference that temperature may play a similar role as vertical stress in 1D consolidation condition to make the soil dense and thus reduce the creep rate.

In general, as the internal structure of the soil becomes denser, the soil particles and aggregates are compressed and recombined, and the total pore volume is supposed to reduce (Zheng et al., 2021). However, it can be found that the number of small-sized pores seems to have become more, and penetrating pores appear when the temperature increases. To quantitatively analyze the pore microscope parameters, Image Pro Plus (IPP) software was adopted to process the SEM photos. The pore size, pore area, mean pore diameter, and fractal dimension have been obtained the results from IPP process. The surface porosity was introduced and defined as the ratio of the total area of pores on a surface to the total area of that surface of the specimen since the photos of specimen in SEM test can be approximated as a flat 2D surface. The surface porosity can be expressed as the following equation

$$N = \frac{S_{pore}}{S_{total}} \tag{14}$$

where N is surface porosity, S_{pore} is the total pore area in the photo after binarization, and S_{total} is the total area of the photo after binarization.

Fig. 17 presents the variations of surface porosity and mean pore diameter with temperature in SEM photos with 1000× magnification. It can be observed that the surface porosity is varied from 15% to 20% and the mean pore diameter ranges from 2.5 to 2.9 μm with different temperature. Since the surface porosity is a two-dimensional parameter that does not consider the depth and direction of pores, it is different from the conventional porosity. Moreover, the surface porosity increases and the mean pore diameter becomes smaller as temperature increases, which means that there is much more small-sized pore in the high temperature treated soil. Combined Fig. 18, it appears that, with temperature increases, the large-sized and middle-sized pores transfer to the small-sized pores owing to the more active microstructure rearrangement. More pores benefit to form drainage channels in the internal structure of soils. It is a possible reason for that why the hydraulic conductivity increases with temperature in addition to the viscosity of the water decreases. The pore area distributions of three HKM D specimens after isothermal oedometer tests are presented in Fig. 18. One can see that the proportion of pores with the area ranging from 0 to 5μm^2 in G1T2 and G1T3 specimens is 12~15% more than that in G1T1 specimen, however, the proportion of pores with the area larger than 10μm^2 is the largest in G1T1 specimen. It is revealed that the small-sized pores are easier to be formed after particle sliding and inner structure rearrangement for soils at high temperatures. The results of SEM tests strongly support the macro consolidation and creep behaviors of HKMD.

Conclusions

The multi-staged oedometer tests with different temperatures were performed to investigate the effects of temperature on the consolidation behavior of the remolded HKMD. The compressibility characteristics, the preconsolidation pressure, and the creep parameters were obtained from the data of oedometer tests. Moreover, the creep behavior was evaluated by using Yin's non-linear creep function and the influences of temperature on the nonlinear parameters were presented. In this study, the main conclusions can be drawn as follows:

(1) Casagrande's logarithmic of time method was used for the t_{EOP} determination. Under any vertical stress, the value of t_{EOP} decreases with the increasing temperature, indicating the

primary consolidation ends prematurely at high temperatures. Correspondingly, the rate of consolidation increases with temperature increases.

(2) The compression index C_c of HKMC is independent of the temperature between 20 to 60 °C, while the swelling index C_s of HKMC slightly decreases after the heating-cooling cycle. Meanwhile, C_s is also related to unloading amplitude: the larger the unloading amplitude, the higher the value of the swelling index.

(3) Due to the decreasing viscosity and unit weight of pore water at high temperatures, the permeability of HKMD increases with an increase in temperature. It is also found that C_k value proposed by Taylor slightly increases with the increasing temperature.

(4) The preconsolidation pressure $\sigma_{zp}^{'}$ decreases as temperature increases. The experimental results showed a good agreement with calculated preconsolidation pressure by utilizing these functions published in the literature with appropriate parameters.

(5) The creep behavior and nonlinear creep of HKMD are temperature and stress-dependent. The creep coefficient, the nonlinear creep parameter, and the creep strain limit gradually decrease with increasing vertical stress and temperature.

(6) SEM photos show that the soil microstructure becomes denser, the interaction is changed to some extent, and the soil particle rearrangement is more complicated when soil is subjected to high temperatures. The quantitative analysis reveals the surface porosity and small-sized pore increase in soil with temperature increases.

Conflict of Interest

No potential conflict of interest was reported by the authors.

Data Availability Statement

All data, models, or codes that support the findings of this study are available from the corresponding author upon reasonable request.

Acknowledgment

This research was funded by an RIF project and a GRF project, grant number R5037-18F and 15210020 from RGC of HKSARG of China; two grants of the Research Institute of Land of Space, The Hong Kong Polytechnic University, grant number CD82 and CD7A; Shenzhen Science and Technology Innovation Commission, grant number JCYJ20210324105210028, the Key Special Project for Introduced Talents Team of Southern Marine Science and Engineering Guangdong Laboratory (Guangzhou), grant number GML2019ZD0210; and the grant of Southern Marine Science and Engineering Guangdong Laboratory (Guangzhou), grant number K19313901.

References

Abuel-Naga, Bergado, D., Bouazza, A., & Ramana, G. (2007). Volume change behaviour of saturated clays under drained heating conditions: experimental results and constitutive modeling. *Canadian Geotechnical Journal, 44*(8), 942-956.

Abuel-Naga, Bergado, D., & Chaiprakaikeow, S. (2006). Innovative thermal technique for enhancing the performance of prefabricated vertical drain during the preloading process. *Geotextiles and Geomembranes, 24*(6), 359-370.

Abuel-Naga, Bergado, D., Soralump, S., & Rujivipat, P. (2005). Thermal consolidation of soft Bangkok clay. *Lowland Technology International, 7*(1, June), 13-21.

Abuel-Naga, H., Bergado, D., Ramana, G., Grino, L., Rujivipat, P., & Thet, Y. (2006). Experimental evaluation of engineering behavior of soft Bangkok clay under elevated temperature. *Journal of Geotechnical and Geoenvironmental Engineering, 132*(7), 902-910.

Amatya, B. L., Soga, K., Bourne-Webb, P. J., Amis, T., & Laloui, L. (2012). Thermo-mechanical behaviour of energy piles. *Geotechnique, 62*(6), 503-519. doi:10.1680/geot.10.P.116

Boudali, M., Leroueil, S., & Srinivasa Murthy, B. (1994). Viscous hebaviour of natural clays. In *International conference on soil mechanics and foundation engineering*.

Burghignoli, A., Desideri, A., & Miliziano, S. (2000). A laboratory study on the thermomechanical behaviour of clayey soils. *Canadian Geotechnical Journal, 37*(4), 764-780.

Campanella, R. G., & Mitchell, J. K. (1968). Influence of temperature variations on soil behavior. *Journal of Soil Mechanics & Foundations Division, 94*(3), 709-734.

Cekerevac, Laloui, L., & Vulliet, L. (2002). Dependency law for thermal evolution of preconsolidation pressure. In *Proceedings of the 8th International Symposium on Numerical Models in Geomechanics, Rome, Italy, Edited by GN Pande and S. Pietruszczak. AA Balkema*.

Cekerevac, C., & Laloui, L. (2004). Experimental study of thermal effects on the mechanical behaviour of a clay. *International Journal for Numerical and Analytical Methods in Geomechanics, 28*(3), 209-228. doi:10.1002/nag.332

Cekerevac, C., Laloui, L., & Vulliet, L. (2002). Dependency law for thermal evolution of preconsolidation pressure. In *Proceedings of the 8th International Symposium on Numerical Models in Geomechanics, Rome, Italy, Edited by GN Pande and S. Pietruszczak. AA Balkema*.

Chen, Z.-J., Feng, W., Li, A., Al-Zaoari, K. Y. M., & Yin, J.-H. (2022). Experimental and molecular dynamics studies on the consolidation of Hong Kong marine deposits under heating and vacuum preloading. *Acta Geotechnica*, 1-15.

Chen, Z.-J., & Yin, J.-H. (2023). A New One-Dimensional Thermal Elastic-Viscoplastic Model for the Thermal Creep of Saturated Clayey Soils. *Journal of Geotechnical and Geoenvironmental Engineering, 149*(4), 04023010.

Chen, Z.-J., Zhao, R.-D., Chen, W.-B., Wu, P.-C., Yin, J.-H., & Feng, W.-Q. (2023). Effects of temperature on the time-dependent compression and shear behaviour of a soft marine clayey soil. *Engineering Geology*, 107005.

Cheng, C. M., & Yin, J. H. (2005). Strain-rate dependent stress-strain behavior of undisturbed Hong Kong marine deposits under oedometric and triaxial stress states. *Marine Georesources & Geotechnology, 23*(1-2), 61-92. doi:10.1080/10641190590953818

Constantz, J. (1982). Temperature dependence of unsaturated hydraulic conductivity of two soils. *Soil Science Society of America Journal, 46*(3), 466-470.

Cui, Y.-J., Le, T. T., Tang, A. M., Delage, P., & Li, X.-L. (2009). Investigating the time-dependent behaviour of Boom clay under thermomechanical loading. *Geotechnique, 59*(4), 319-329.

Davies, T., & Banerjee, P. (1980). *Constitutive relationships for ocean sediments subjected to stress and temperature gradients*: United Kingdom Atomic Energy Authority.

Delage, P., Jun, C. Y., & Sultan, N. (2004). On the thermal behaviour of Boom clay. In *Proceedings Eurosafe 2004 Conference*, Berlin.

Delage, P., Sultan, N., Cui, Y.-J., & Ling, L. X. (2011). Permeability changes in Boom clay with temperature. *arXiv preprint arXiv:1112.6396*.

Delage, P., Sultan, N., & Cui, Y. J. (2000). On the thermal consolidation of Boom clay. *Canadian Geotechnical Journal, 37*(2), 343-354.

Eriksson, L. (1989). Temperature effects on consolidation properties of sulphide clays. In *International Conference on Soil Mechanics and Foundation Engineering: 13/08/1989-18/08/1989*.

Fang, Z., & Yin, J. H. (2006). Physical modelling of consolidation of Hong Kong marine clay with prefabricated vertical drains. *Canadian Geotechnical Journal, 43*(6), 638-652. doi:10.1139/T06-021

Feng, W. Q., Lalit, B., Yin, Z.-Y., & Yin, J.-H. (2017). Long-term non-linear creep and swelling behavior of Hong Kong marine deposits in oedometer condition. *Computers and Geotechnics, 84*, 1-15.

Feng, W. Q., & Yin, J. H. (2017). A new simplified Hypothesis B method for calculating consolidation settlements of double soil layers exhibiting creep. *International Journal for Numerical and Analytical Methods in Geomechanics, 41*(6), 899-917. doi:10.1002/nag.2635

Fox, P. J., & Edil, T. B. (1996). Effects of stress and temperature on secondary compression of peat. *Canadian Geotechnical Journal, 33*(3), 405-415.

Green, W. J. (1969). *The influence of several factors on the rate of secondary compression of soil.* (Master Thesis). University of Missouri,

Gupta, B. (1964). *Creep of saturated soil at different temperatures.* (Master Thesis). University of British Columbia,

Habibagahi, K. (1977). Temperature effect and the concept of effective void ratio. *Indian Geotechnical Journal, 7*(1), 14-34.

Hillel, D. (1980). *Fundamentals of soil physics*: Academic Press.

Hong, P. Y., Pereira, J. M., Tang, A. M., & Cui, Y. J. (2013). On some advanced thermo-mechanical models for saturated clays. *International Journal for Numerical and Analytical Methods in Geomechanics, 37*(17), 2952-2971. doi:10.1002/nag.2170

Hueckel, T., & Borsetto, M. (1990). Thermoplasticity of Saturated Soils and Shales - Constitutive-Equations. *Journal of Geotechnical Engineering-Asce, 116*(12), 1765-1777. doi:Doi 10.1061/(Asce)0733-9410(1990)116:12(1765)

Jarad, N., Cuisinier, O., & Masrouri, F. (2019). Effect of temperature and strain rate on the consolidation behaviour of compacted clayey soils. *European Journal of Environmental and Civil Engineering, 23*(7), 789-806.

Kaddouri, Z., Cuisinier, O., & Masrouri, F. (2019). Influence of effective stress and temperature on the creep behavior of a saturated compacted clayey soil. *Geomechanics for Energy and the Environment, 17*, 106-114. doi:10.1016/j.gete.2018.09.002

Knellwolf, C., Peron, H., & Laloui, L. (2011). Geotechnical Analysis of Heat Exchanger Piles. *Journal of Geotechnical and Geoenvironmental Engineering, 137*(10), 890-902. doi:10.1061/(Asce)Gt.1943-5606.0000513

Koutsoftas, D. C., Foott, R., & Handfelt, L. D. (1987). Geotechnical Investigations Offshore Hong-Kong. *Journal of Geotechnical Engineering-Asce, 113*(2), 87-105. doi:Doi 10.1061/(Asce)0733-9410(1987)113:2(87)

Le, T. M., Fatahi, B., Khabbaz, H., & Sun, W. (2017). Numerical optimization applying trust-region reflective least squares algorithm with constraints to optimize the non-linear creep parameters of soft soil. *Applied Mathematical Modelling, 41*, 236-256.

Li, Y., Dijkstra, J., & Karstunen, M. (2018). Thermomechanical creep in sensitive clays. *Journal of Geotechnical and Geoenvironmental Engineering, 144*(11), 04018085.

Lingnau, B. E., Graham, J., Yarechewski, D., Tanaka, N., & Gray, M. N. (1996). Effects of temperature on strength and compressibility of sand-bentonite buffer. *Engineering Geology, 41*(1-4), 103-115. doi:Doi 10.1016/0013-7952(95)00028-3

Mitchell, J. K., & Soga, K. (1976). *Fundamentals of soil behavior* (Vol. 3): John Wiley & Sons New York.

Mohajerani, M., Delage, P., Monfared, M., Tang, A. M., Sulem, J., & Gatmiri, B. (2011). Oedometric compression and swelling behaviour of the Callovo-Oxfordian argillite. *International Journal of Rock Mechanics and Mining Sciences, 48*(4), 606-615. doi:10.1016/j.ijrmms.2011.02.016

Morin, R., & Silva, A. J. (1984). The Effects of High-Pressure and High-Temperature on Some Physical-Properties of Ocean Sediments. *Journal of Geophysical Research, 89*(Nb1), 511-526. doi:DOI 10.1029/JB089iB01p00511

Moritz, L. (1995). *Geotechnical properties of clay at elevated temperatures*. Statens geotekniska institut.

Nakase, A., Kamei, T., & Kusakabe, O. (1988). Constitutive Parameters Estimated by Plasticity Index. *Journal of Geotechnical Engineering-Asce, 114*(7), 844-858. doi:Doi 10.1061/(Asce)0733-9410(1988)114:7(844)

Ogawa, A., Takai, A., Shimizu, T., & Katsumi, T. (2020). Effects of temperature on consolidation and consistency of clayey soils. In *E3S Web of Conferences*.

Romero, E., Gens, A., & Lloret, A. (2001). Temperature effects on the hydraulic behaviour of an unsaturated clay. In *Unsaturated soil concepts and their application in geotechnical practice* (pp. 311-332): Springer.

Shahrokhabadi, S., Cao, T. D., & Vahedifard, F. (2020). Thermal effects on hydromechanical response of seabed-supporting hydrocarbon pipelines. *International Journal of Geomechanics, 20*(1), 04019143.

Shi, X. S., Yin, J. H., Feng, W. Q., & Chen, W. B. (2018). Creep Coefficient of Binary Sand-Bentonite Mixtures in Oedometer Testing Using Mixture Theory. *International Journal of Geomechanics, 18*(12), 04018159.

Tang, A. M., Cui, Y. J., & Barnel, N. (2008). Thermo-mechanical behaviour of a compacted swelling clay. *Geotechnique, 58*(1), 45-54. doi:10.1680/geot.2008.58.1.45

Taylor, D. W. (1948). *Fundamentals of soil mechanics* (Vol. 66): LWW.

Tidfors, M., & Sällfors, G. (1989). Temperature effect on preconsolidation pressure. *Geotechnical Testing Journal, 12*(1), 93-97.

Tong, F., & Yin, J.-H. (2011). Nonlinear creep and swelling behavior of bentonite mixed with different sand contents under oedometric condition. *Marine Georesources & Geotechnology, 29*(4), 346-363.

Towhata, I., Kuntiwattanaku, P., Seko, I., & Ohishi, K. (1993a). Volume change of clays induced by heating as observed in consolidation tests. *Soils and Foundations, 33*(4), 170-183.

Towhata, I., Kuntiwattanaku, P., Seko, I., & Ohishi, K. (1993b). Volume change of clays induced by heating as observed in consolidation tests. *Soils Foundations, 33*(4), 170-183.

Tsutsumi, A., & Tanaka, H. (2012). Combined effects of strain rate and temperature on consolidation behavior of clayey soils. *Soils and Foundations, 52*(2), 207-215. doi:10.1016/j.sandf.2012.02.001

Wu, P.-C., Feng, W.-Q., & Yin, J.-H. (2020). Numerical study of creep effects on settlements and load transfer mechanisms of soft soil improved by deep cement mixed soil columns under embankment load. *Geotextiles and Geomembranes, 48*(3), 331-348.

Yin, J. H. (1999a). Non-linear creep of soils in oedometer tests. *Geotechnique, 49*(5), 699-707. doi:DOI 10.1680/geot.1999.49.5.699

Yin, J. H. (1999b). Properties and behaviour of Hong Kong marine deposits with different clay contents. *Canadian Geotechnical Journal, 36*(6), 1085-1095. doi:DOI 10.1139/cgj-36-6-1085

Yin, J. H., & Feng, W. Q. (2017). A new simplified method and its verification for calculation of consolidation settlement of a clayey soil with creep. *Canadian Geotechnical Journal, 54*(3), 333-347. doi:10.1139/cgj-2015-0290

Yin, J. H., & Graham, J. (1989). Viscous-Elastic-Plastic Modeling of One-Dimensional Time-Dependent Behavior of Clays. *Canadian Geotechnical Journal, 26*(2), 199-209. doi:DOI 10.1139/t89-029

Yin, J. H., & Graham, J. (1994). Equivalent Times and One-Dimensional Elastic Viscoplastic Modeling of Time-Dependent Stress-Strain Behavior of Clays. *Canadian Geotechnical Journal, 31*(1), 42-52. doi:DOI 10.1139/t94-005

Zhang, C. L., Rothfuchs, T., Su, K., & Hoteit, N. (2007). Experimental study of the thermo-hydro-mechanical behaviour of indurated clays. *Physics and Chemistry of the Earth, 32*(8-14), 957-965. doi:10.1016/j.pce.2006.04.038

Zheng, Y., Sun, H., Hou, M., & Ge, X. (2021). Microstructure evolution of soft clay under consolidation loading. *Engineering Geology, 293*, 106284.

Zhu, J. G., Yin, J. H., & Luk, S. T. (1999). Time-dependent stress-strain behavior of soft Hong Kong marine deposits. *Geotechnical Testing Journal, 22*(2), 118-126.

Table 1. Physical properties of HKMD

Properties	Value
Specific gravity, G_s	2.65
Water content, w (%)	49-51
Liquid limit, w_L (%)	59
Plastic limit, w_P (%)	23.8
Plastic index, I_P (%)	35.2
Initial void ratio, e_0	1.29-1.31

Table 2. Loading procedures and temperatures in oedometer test

Loading (kPa)	Duration of Group 1 (day)	Duration of G2T1 (day)	Duration of G2T2 (day)
2.5	-	1 (20℃)	1
5	1	1 (20℃)	1
10	1	1 (20℃)	1
20	1	1 (20℃)	1
50	7	1 (30℃)	7
100	7	10 (40℃)	10
200	7	10 (50℃)	10
400	7	-	-
200	0.1	-	-
100	0.1	0.1 (20℃)	0.1
50	0.1	0.1 (20℃)	0.1
100	0.1	0.1 (20℃)	0.1
200	0.1	0.1 (20℃)	0.1
400	0.1	10 (30 ℃)	10
800	7	7 (40 ℃)	7
1600	7	10 (50 ℃)	10
Total	45.6	52.4	58.4

Group 1 includes G1T1, G1T2, and G1T3.

List of Figure

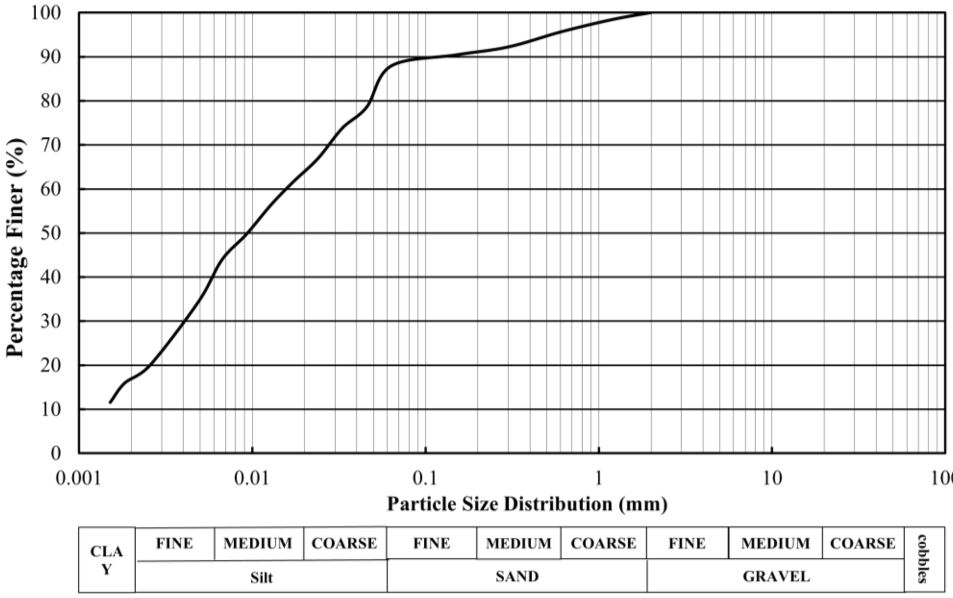

Fig. 1 Particle size distribution curve of HKMD

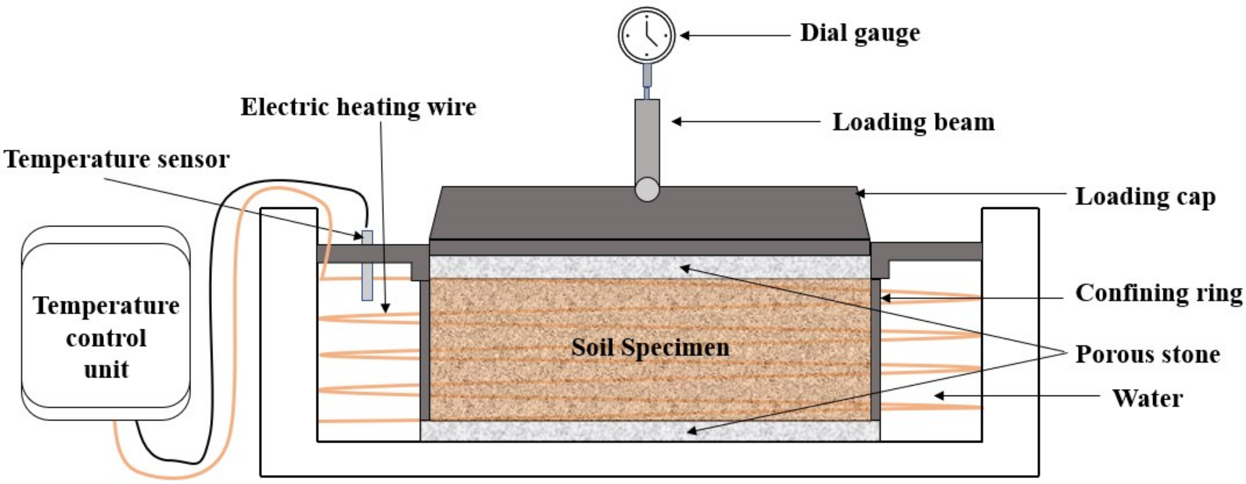

Fig. 2 Schematic drawing of the modified temperature-controlled oedometer

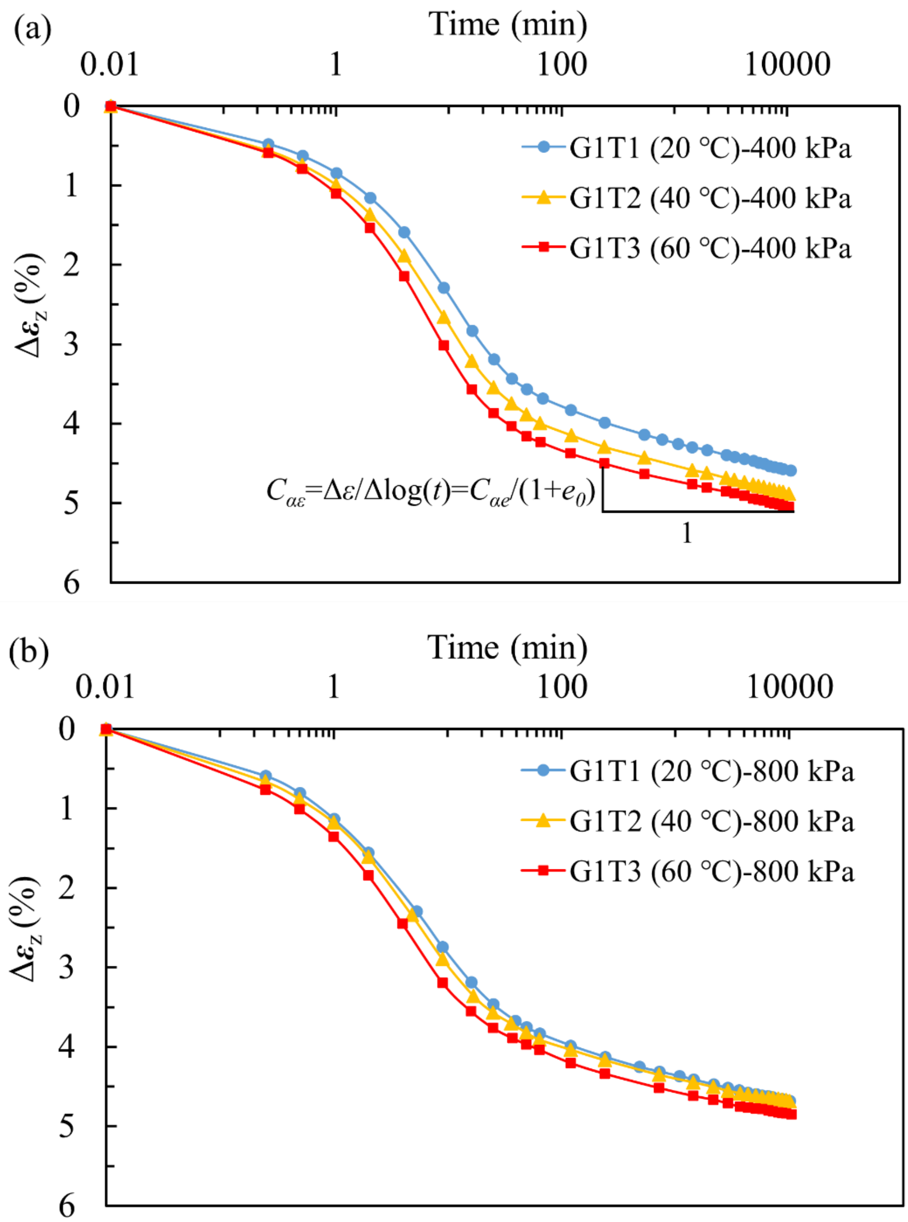

Fig. 3 The relationship between the incremental vertical strain and *log(t)* of three isothermal tests: (a) under the vertical stress of 400 kPa, (b) under the vertical stress of 800 kPa

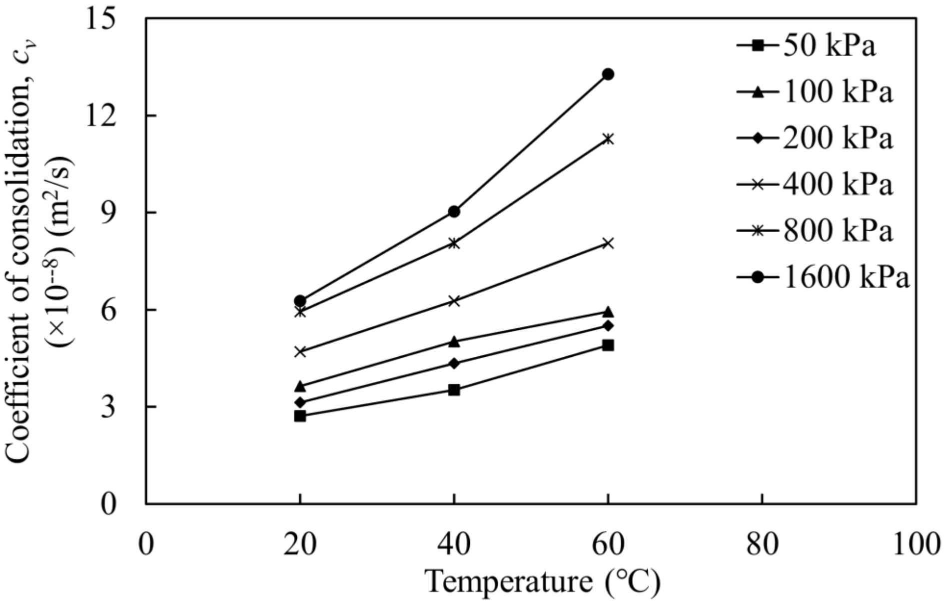

Fig. 4 Evolution of coefficient of consolidation c_v with temperature under different vertical stresses

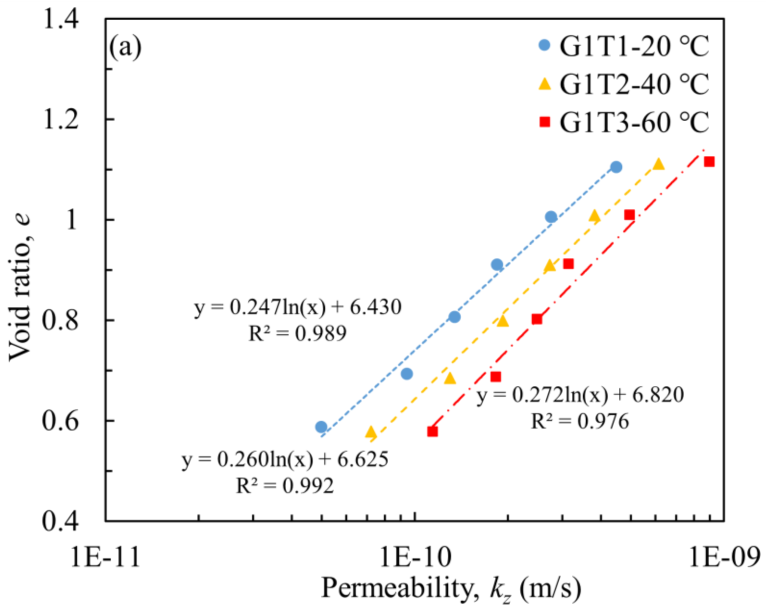

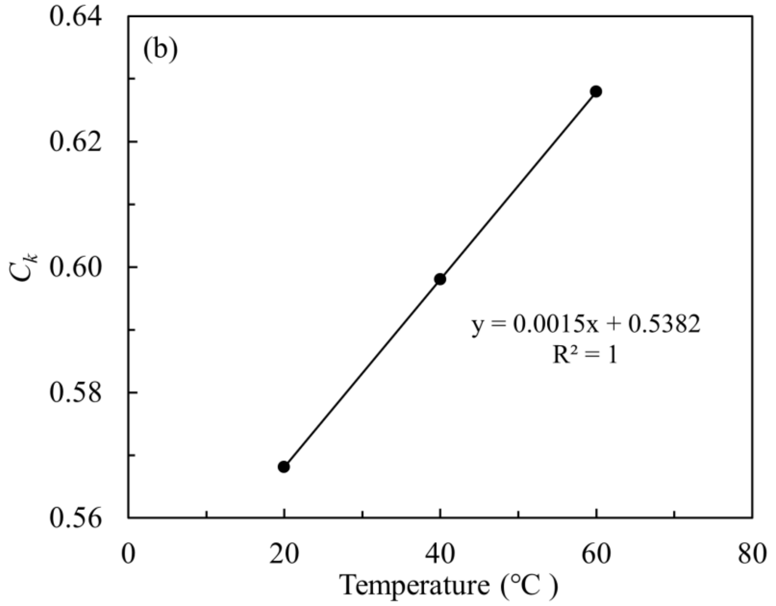

Fig. 5 (a) Variation of permeability with void ratio, (b) variation of C_k with temperature

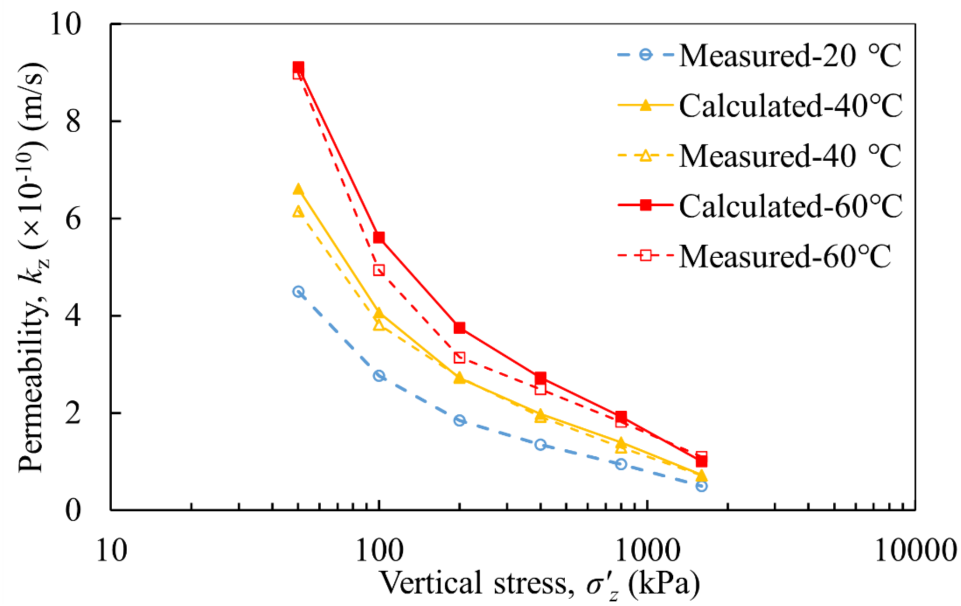

Fig. 6 Comparison between the values of permeability obtained from the calculation and experimental data

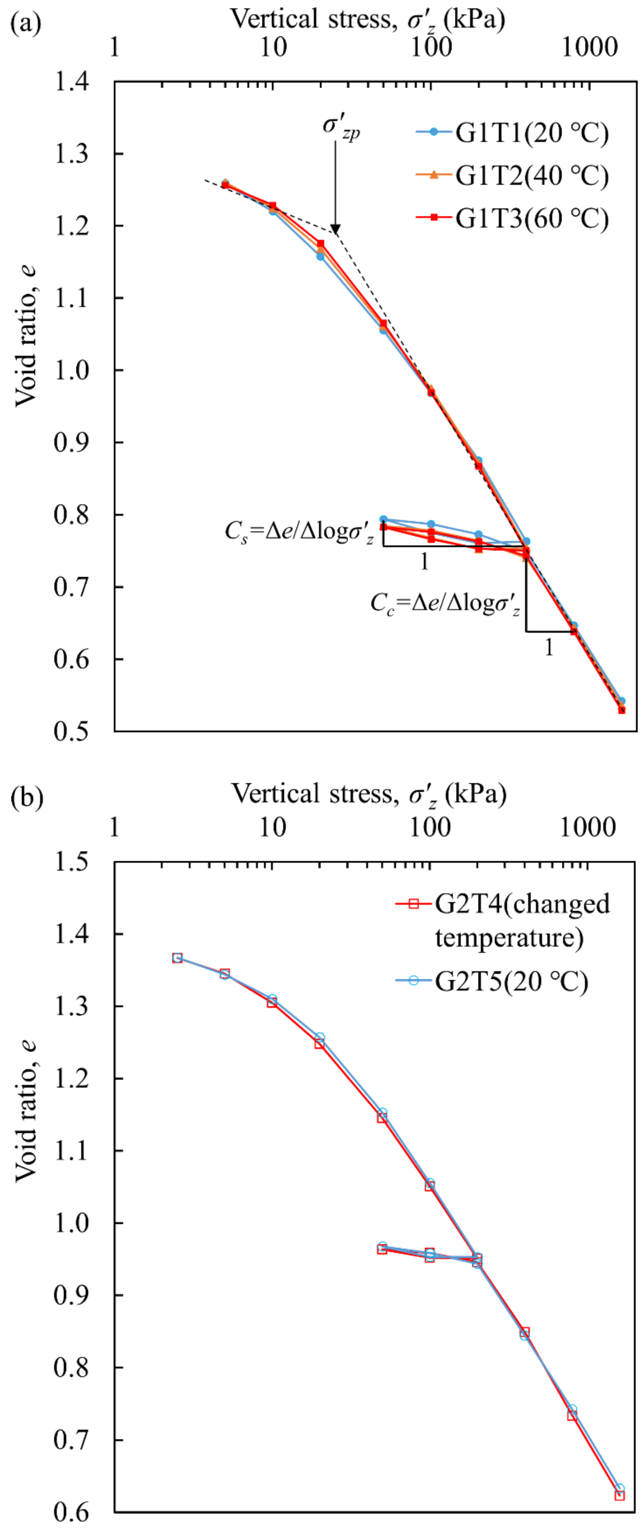

Fig. 7 The curves of void ratio *versus* logarithm vertical stress (e-logσ'_z) at t_{EOP}: (a) Group 1 and (b) Group 2

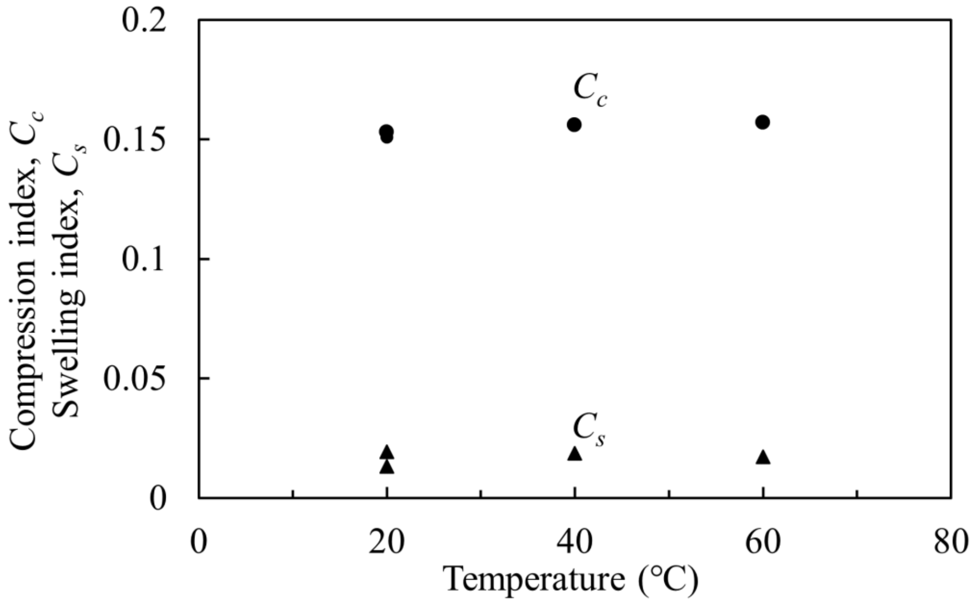

Fig. 8 Evolution of the compression index and the swelling index with an increase in temperature

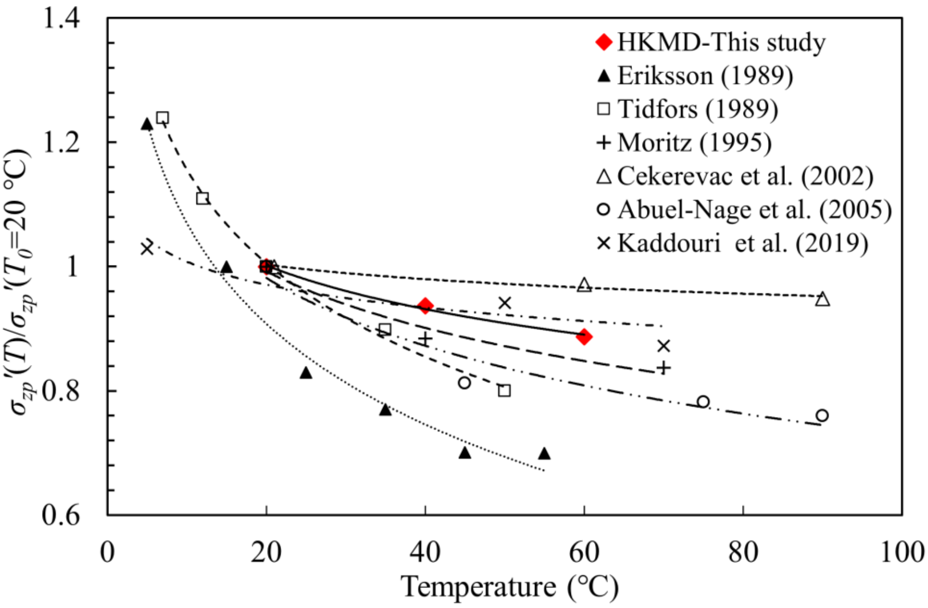

Fig. 9 Variation of normalized preconsolidation pressure with temperature

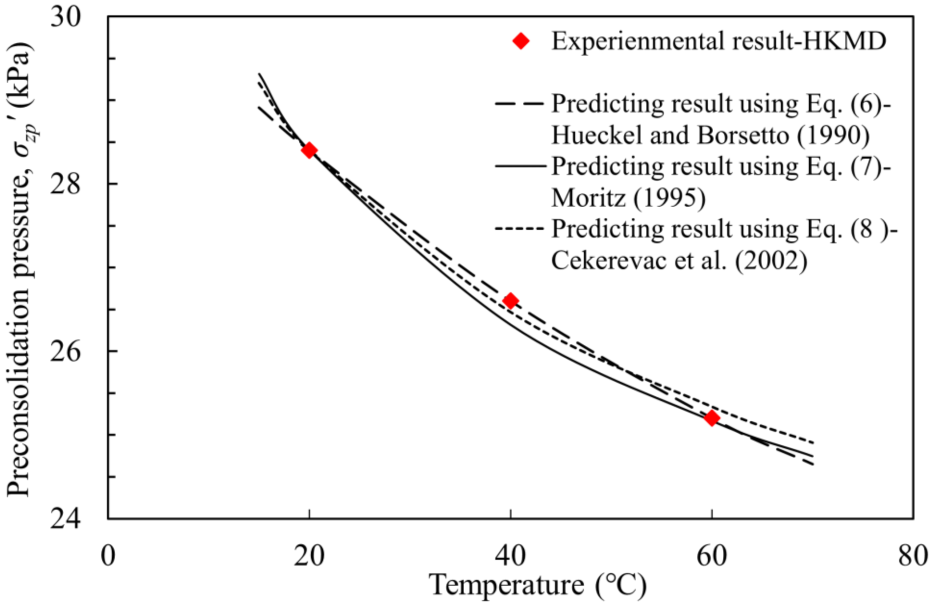

Fig. 10 Comparison between the predicted results using three different equations and the oedometer test results

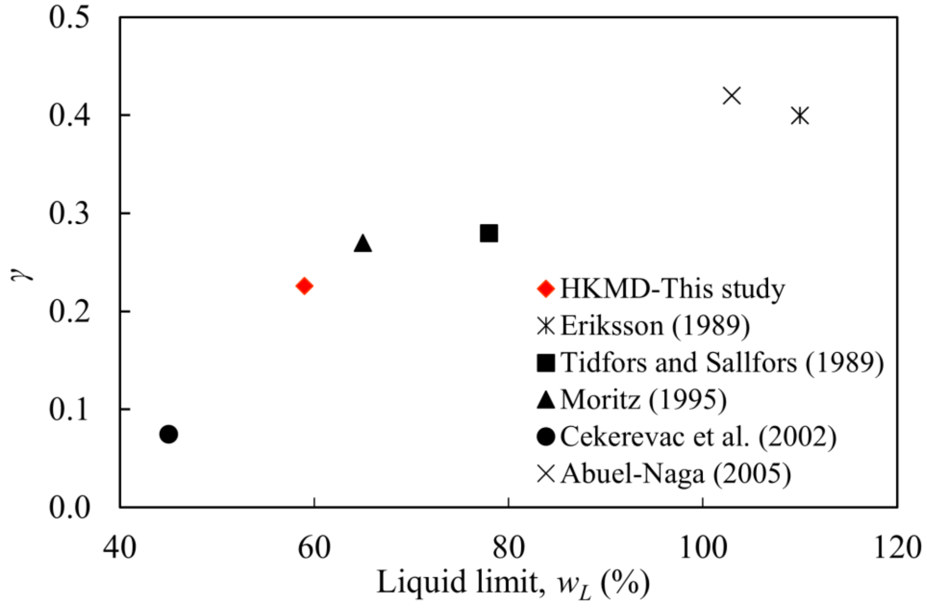

Fig. 11 Evolution of modeling parameter γ with liquid limit for different soils

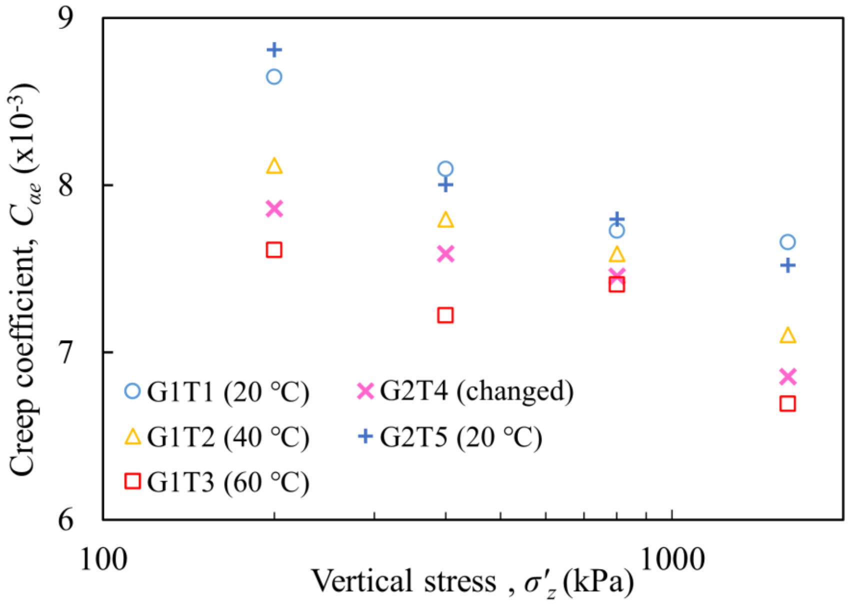

Fig. 12 Relationship between creep coefficient and vertical stress for isothermal oedometer tests

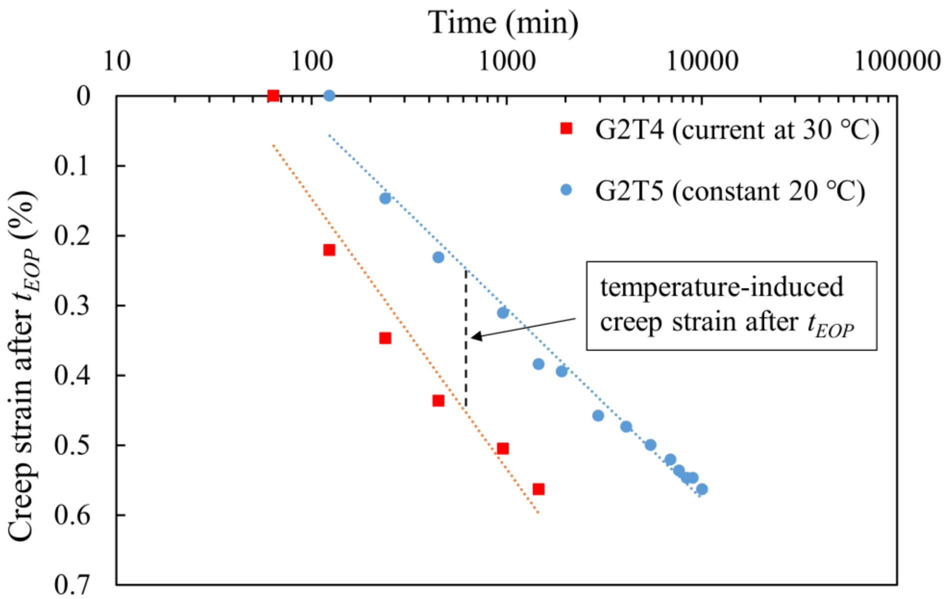

Fig. 13 Creep strain after t_{EOP} of G2T4 and G2T5 with time under vertical stress of 50 kPa

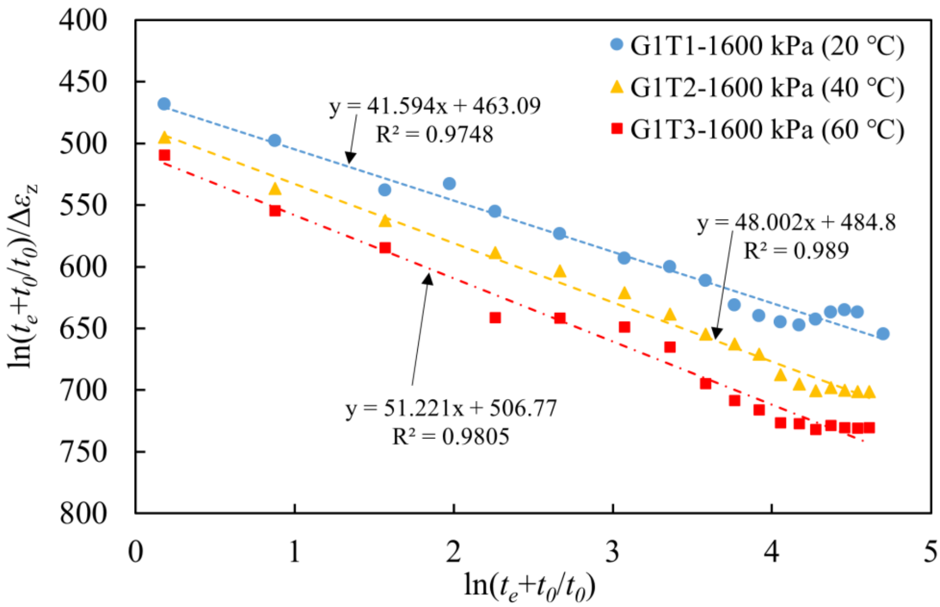

Fig. 13 Representative curve fitting for non-linear creep function of specimens in Group 1 under effective stress of 1600 kPa

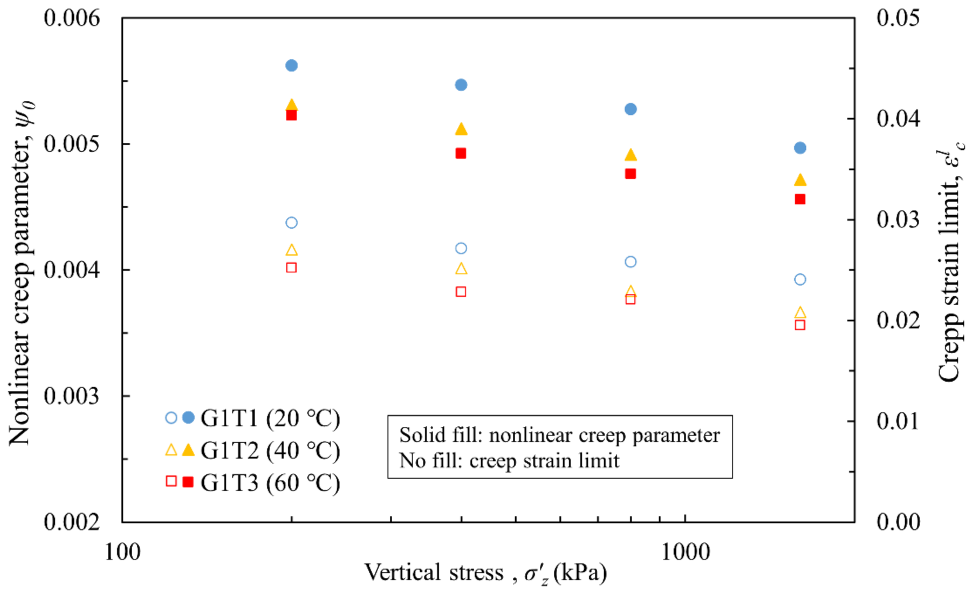

Fig. 14 Evolution of parameters in nonlinear creep function

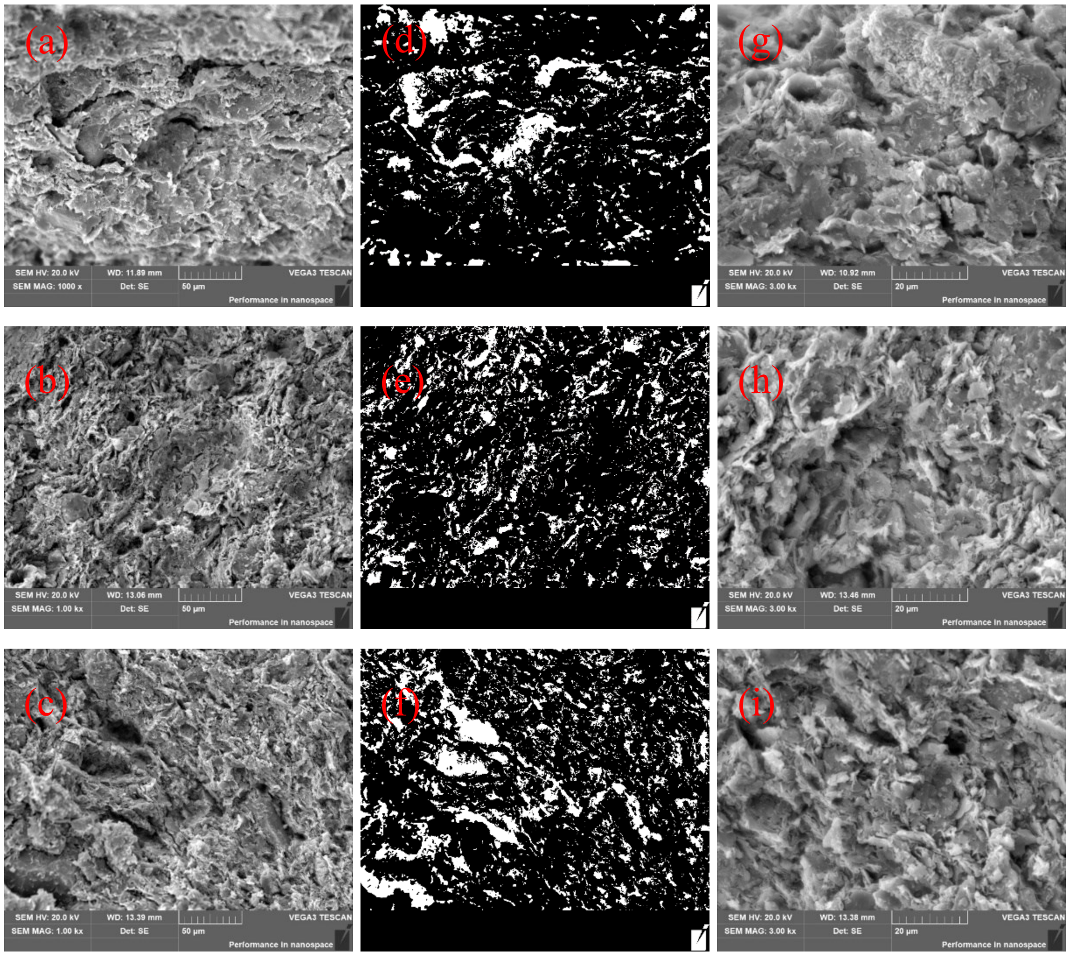

Fig. 15 SEM photos of HKMD specimens after oedometer tests: (a)-(c) specimens at 20, 40, and 60 ℃ with 1000× MAG; (d)-(f): (a)-(c) after binarization; (g)-(i) specimens at 20, 40, and 60 ℃ with 3000× MAG

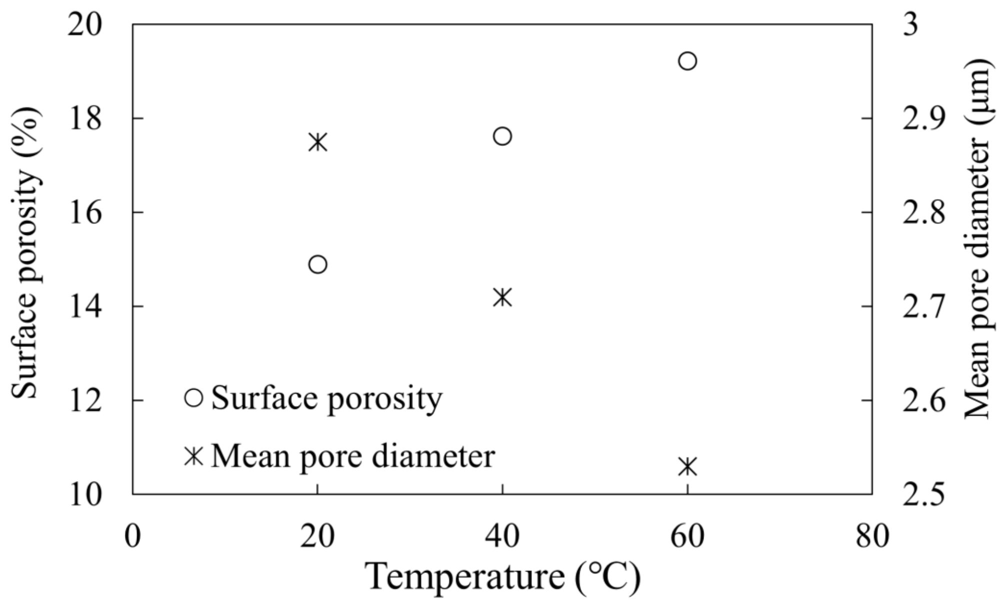

Fig. 16 The variations of surface porosity and mean pore diameter with temperature

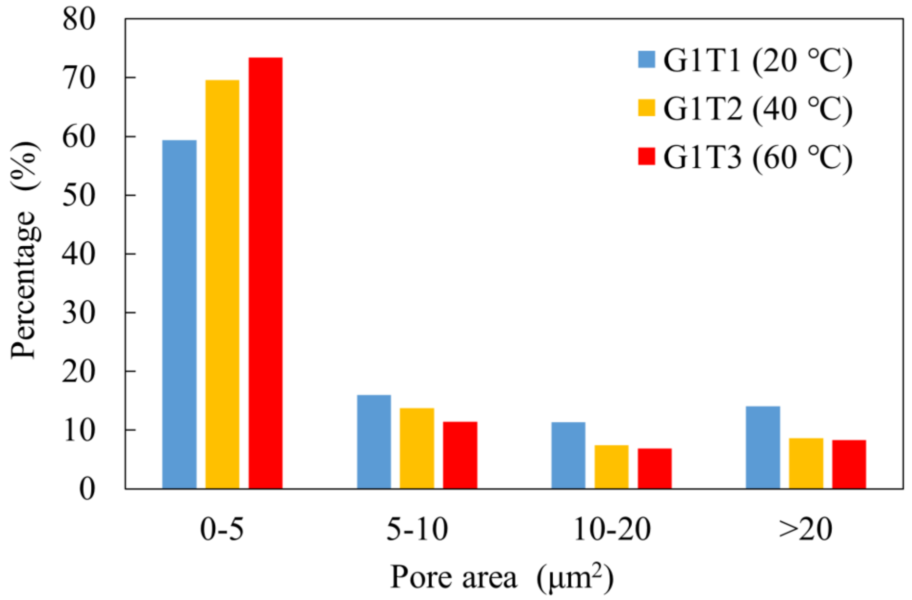

Fig. 17 Pore size distribution of HKMD specimens after oedometer tests at different temperatures